Upgrading biogas to a bio-methane by use of nano-structured ceramic membranes.

OGUNLUDE, P., ABUNUMAH, O., ORAKWE, I., SHEHU, H., MUHAMMAD-SUKKI, F., and GOBINA, E.

2019

UPGRADING BIOGAS TO A BIO-METHANE BY USE OF NANO-STRUCTURED CERAMIC MEMBRANES

Priscilla Ogunlude, Ofasa Abunumah, Ifeyinwa Orakwe, Habiba Shehu, Firdaus Muhammad-Sukki and Edward Gobina

Department Centre for Process Integration and Membrane Technology, School of Engineering, Robert Gordon University, Sir Ian Wood Building, Garthdee Road, ABERDEEN AB10 7GJ

ABSTRACT: In order to meet the demands of growing economies while considering environmental implications, the use of clean and renewable sources of energy has increasingly become of interest. Biogas utilisation is a means by which these rising needs can be met. This involves the use of waste materials; which are deposited on a daily basis by agriculture, sewage, household, to produce energy that may be used for heating, electricity, transportation and other daily needs. This paper would look into the use of nano-structured ceramic membranes for the upgrading of biogas to a high value fuel that can be used for a variety of purposes. The use of membranes offers great advantages including low running costs, high efficiency and the elimination of the need for phase change of the gas. Experiments were carried out using membranes of different pore sizes - 15nm, 200nm and 6000nm to ascertain which would be the most suitable for use in terms of permeability and yield of product gas. The 15nm membrane showed the greatest exit flow of methane compared to carbon dioxide and a mechanism approaching an ideal knudsen regime. Taking into account the effect of molecular weight and viscosity, these results show that the smallest membrane pore size of 15nm had a greater impact on the flow mechanism and thus improvement can be made by modification of the membrane to achieve a mechanism of surface diffusion of the particles.

Keywords: biogas, upgrading, renewable, nano-structured, ceramic, membrane

1. INTRODUCTION

Biogas is evolved from the anaerobic digestion of bio-gradable materials such as human or animal waste, food scraps, cotton, wool, wood and other organic sources. The biogas obtained can be used directly as a fuel but in order to fully harness its potential, it is cleaned and upgraded to a point where its heating value is very high, and impurities are removed such that it can be injected into the national gas grid.

The treatment or upgrading of biogas is essential because: (i) the presence of CO_2 in the gas reduces the power output from the engine, takes up space when biogas is compressed for storage and causes freezing problems when the compressed gas undergoes expansion at valves and metering points (ii) traces of H_2S can produce H_2SO_4 which corrode pipes, fittings, etc. (iii) moisture reduces the heating value of the biogas and causes corrosion. Nonetheless, several safety aspects need to be considered

during the treatment and utilization of biogas. It is very crucial to be aware of the associated risks and to minimize them. The most common risks include flammability, poisoning (due to the presence of H_2S), suffocation and the risks associated with high pressures and temperatures. On the other hand, the advantage is that biogas is lighter than air and any gas leakage would rise upward. Also, upgraded biogas has a greater temperature of ignition than both petrol and diesel so the possibility of a fire or explosion is reduced (1).

The advantages of utilizing biogas are numerous. Research has proven that upgraded biogas shows lower carbon intensities compared to other vehicle fuel (2,3). Currently, American liquified natural gas (i.e. methane) is being exported to counties like China, India and Japan who still rely on coal for power generation but wish to substitute their "dirty" coal for clean gas (4). Thus, this technology can be implemented on a large scale for the export of upgraded biogas to other countries without knowledge, infrastructure and expertise, this would provide revenue for the economy as well as an abundance of jobs. This highlights one of the advantages of biogas compared to other forms of renewable energy such as solar and wind that cannot be stored and transported.

This research would introduce a novel method for the upgrading of biogas to a clean and useful fuel replacing fossil fuels. The use of nano-structured membrane technology would be implemented, where biogas components pass through the membrane as the feed gas to observe the separation characteristics at various operating conditions of pressure and temperature for three different membrane pore sizes. One of the prime goals is to demonstrate long term performance and reliability under simulated industrial conditions.

The main objectives are:

1. To reduce greenhouse gas emissions and the effect of global warming by utilizing biogas. This is clean and renewable source of energy.

2. To harness biogas as source of energy and lessen reliance on other fossil fuels. This would also reduce the cost of importation of fossil fuels since biogas is available in abundance

3. To create wealth from waste by upgrading biogas generated from organic waste materials

4. To increase the efficiency of the overall process in terms of energy consumption, purity and recovery of bio-methane produced.

2. LITERATURE REVIEW

2.1 Current Technologies

Figure 1 shows the current state-of-the-art technologies for biogas upgrading. Four technologies are currently being used to upgrade biogas to biomethane. These include absorption, adsorption, membrane separation and cryogenic separation.
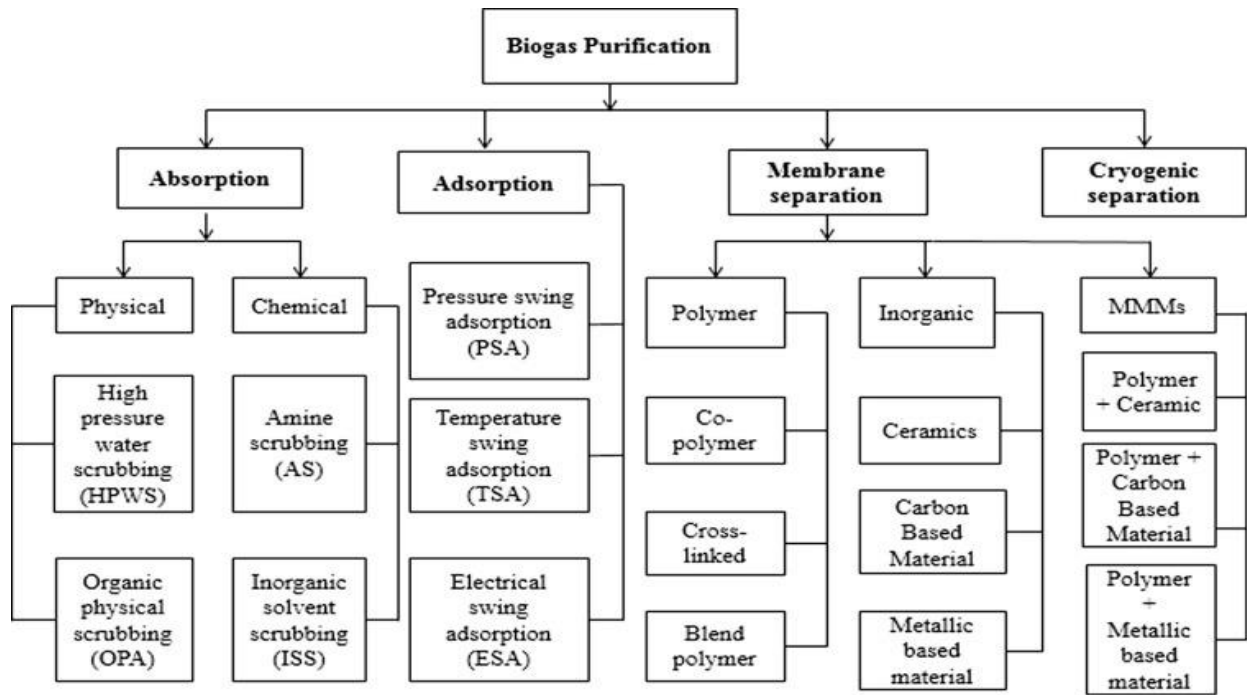
Figure 1 Current Technologies for Biogas Upgrading (5)

The current methods of upgrading biogas have numerous disadvantages. For instance, to remove CO_2, scrubbers may be used but this results in a significant amount of waste products that need to be properly disposed of thereby increasing costs. In this research, the use of membrane technology is explored as an effective and efficient means of upgrading biogas.

In the use of membranes, the energy consumption is relatively lower than the conventional upgrading processes as they do not consume energy in the latent heat of evaporation and the possibility of methane slip or losses is minimal. Other advantages are that they are compatible with temperature sensitive materials and are not chemically altered, separation does not involve phase change, there is a higher efficiency of separation, they are simple to operate membranes have high selectivity and permeation rate (6).

2.2 Membrane Gas Transport Mechanisms

The mechanism of gas transport in membranes are derived from Graham's law and Fick's law (7). Graham's law states that the rate of diffusion of a gas is inversely proportional to the square root of its molecular weight. In mathematical form (8):

$$\frac{Rate\ a}{Rate\ b} = \left(M_b/M_a\right)^{1/2} \qquad (1)$$

Where,
Rate a and Rate b denote the rate of diffusion of the first gas and second gas respectively,
M_a and M_b are the molar masses of gases a and b in g mol^{-1} respectively.
Fick's law relates the molar flux to the concentration gradient through the membrane thickness. This can be written in mathematical form as (8):

$$F_i = \frac{P_e}{L}(P_1 - P_2)A \qquad \left(\frac{mol}{s}\right) \qquad (2)$$

Where,
P_e is the permeability, mol m^{-1} s^{-1} Pa^{-1}

L is the length, m

P_1, P_2 is the pressure at point 1 and 2 respectively, Pa

A is the permeation area, m²

Gas transport in membranes can take place through several mechanisms including Hagen-Poiseuille flow, Knudsen diffusion, surface diffusion, capillary condensation and molecular sieving.

2.2.1 Hagen-Poiseuille

This mechanism comes to play when the pore diameter is large compared to the mean free path of the gas molecules (λ). Here, the gas permeance is inversely proportional to the gas viscosity (8,9).

$$P_e = \frac{\varepsilon \eta r^2}{8 \mu RT} P_{av} \quad \text{(mol m}^{-1}\text{ s}^{-1}\text{ Pa}^{-1}\text{)} \tag{3}$$

Where,

Ɛ is the porosity, dimensionless

μ is the viscosity, Pa s

η is the shape factor assumed equal to the reciprocal tortuosity, dimensionless

R is the universal gas constant, J K^{-1} mol^{-1}

r is the pore radius, m

T is the temperature, K

P_{av} is the mean pressure, Pa

2.2.2 Knudsen Diffusion

This may occur when the pore size is larger than that of the gas molecules but smaller than its mean free path (λ). There is elastic collision between the gas molecules and the pore wall and therefore no interaction between them. The permeance is given as (8,9):

$$P_e = \frac{2 \varepsilon \eta r v}{3RT} \quad \text{(mol m}^{-1}\text{ s}^{-1}\text{ Pa}^{-1}\text{)} \tag{4}$$

Where,

Ɛ is the porosity, dimensionless

η is the shape factor assumed equal to the reciprocal tortuosity, dimensionless

r is the pore radius, m

v is the molecular velocity, ms^{-1}

R is the universal gas constant, J K^{-1} mol^{-1}

T is the temperature, K

2.2.3 Surface Diffusion

This occurs at low temperatures where contact between the gas molecules and inner surface is so strong compared to their kinetic energy such that the molecules cannot escape. The permeance is given as (8,9):

$$P_{SD} = P_O \exp\left(\frac{-\Delta Ha - \Delta Esd}{RT}\right) \tag{5}$$

Where,

P_0 is the pressure, Pa

$(-\Delta Ha - \Delta Esd)$ is the energy barrier for diffusing molecules to permeate through the membrane, J m^{-1} s^{-1}

R is the universal gas constant, J K^{-1} mol^{-1}

T is the temperature, K

2.2.4 Capillary Condensation

Capillary condensation usually occurs at higher gas pressures with temperatures lower than the critical temperature. Therefore, condensed gas molecules are transported across the pores of the membrane (10,11):

$$\frac{\rho RT}{M} \ln \frac{P_t}{P_o} = -\frac{2\sigma cos\theta}{r} \tag{6}$$

Where,

ρ is the density, kg/m^3

M is the gas molecular weight, kg mol^{-1}

θ is the contact angle

P_t is the total pressure, Pa

σ is the interfacial tension, N/m

r is the radius, m

R is the universal gas constant, J K^{-1} mol^{-1}

T is the temperature, K

P_o is the vapor pressure, Pa

2.2.5 Molecular Sieving

This mechanism separates the molecules by their size using membrane pores of similar size of the molecules. The typical pore sizes for molecular sieving are less than 2nm (12,13).

$$J_s\,(T)\sim\rho q_{sat} D_S^O\,(0)(1-\theta)^{-1}\,\exp\,(-E_{D,S}/RT)d\theta/dx. \tag{7}$$

Where,

$J_s(T)$ is the flux at temperature T, mol/s

ρ is the density, kg/m^3

q_{sat} is the saturated molar volume, m^3/mol

$D_s^o(0)$ is the limiting surface diffusivity, m^2/s

θ is the fraction of available adsorption sites that are occupied, dimensionless

$E_{D,S}$ is the surface diffusion activation energy, kJ/mol

R is the universal gas constant, J K^{-1} mol^{-1}

T is the temperature, K

Figure 2 describes the various gas transport mechanisms occurring in the different types of membrane pore sizes with their perm-selectivities.

Type of Membrane	Transport Mechanism	Perm-Selectivity $(\alpha^*_{A/B})$
Macroporous > 50 nm	Viscous flow	1
	Molecular diffusion	1
Mesoporous, 2–50 nm	Knudsen diffusion	$\sqrt{\frac{M_B}{M_A}}$
	Surface diffusion	More than Knudsen value
	Capillary Condensation, pore filling	Much more than Knudsen value
Microporous, <2 nm	Micropore diffusion	Much more than Knudsen value

(*) $\alpha_{A/B}$ is defined as the perm-selectivity of compound A over B. In the case of Knudsen mechanism, it is equal to the square root of the reverse of the molecular weights of compounds A and B (M_A and M_B).

Figure 2. Gas transport mechanism in porous materials and their perm-selectivity (14)

3. METHODOLOGY

This research involved the use of a shell-and-tube system. Three (3) different membrane modules of different pore sizes were studied with the membrane fitted into center of the tube covered with graphite seals. Methane and carbon dioxide gases analyzed under different temperatures and pressures.

3.1 Experimental Set-up

The experimental set-up used in this work is shown in the figure 3. This set-up contains a gas cylinder (4) with regulator (3) which contains the feed gas, this can be sent to the membrane. It contains a heat regulator (5), pressure gauge (1), temperature indicator (7), volumetric meter (6), the membrane module that has been sealed to prevent leakage of gas and covered in heating tape with insulation (2) with an exit line through which the outlet gas flows to the fume cupboard. This chamber was set up to determine the flux of each gas through the membrane under different operating conditions.

.

Figure 3 Experimental set-up showing all equipment including; pressure gauge(1), membrane module covered with heating tape(2), gas regulator(3), gas cylinder(4), heat regulator(5), volumetric meter(6) and temperature indicator(7)

Figure 4 shows different views of a membrane used.

Figure 4 Top view (above) and side view (below) of a membrane.

3.2 Experimental Procedure

A leak test was conducted prior to each experiment. At the inlet, the methane gas to be analysed was fed in at a predetermined pressure and readings were recorded while operating at thermal stability of 20ºC, 50ºC, 70ºC and 100ºC respectively. The stability of the flow meter confirmed that a steady constant driving force was being maintained.

At the outlet, there was also a flow meter to measure the flow of the outgoing gas. The flux was then obtained given that both inlet and outlet flow rates were measured. The experiment was carried out at 0.2, 0.6, 1.0, 1.4, 1.8, 2.2, 2.6 and 3.0 bar.

The membrane module was flushed prior to changing the type of gas flowing through e.g. to enable us to measure the flow characteristics of carbon dioxide gas by repeating the procedure. By comparing the flow characteristics of the different gases, the perm-selectivity of the membrane was measured.

Additionally, to note how the membrane module would separate the two gases, a gas mixture containing a known composition of both gases and maintained at a set pressure would be analysed by passing the mixture through the chamber to measure the total permeation across the module and measuring how fast the outlet pressure increases. By checking the outlet gas composition, we would also measure how much of the exit gas from the total permeation is methane versus carbon dioxide which would enable us to figure out how well the membrane will separate the gases in an industrial application.

4. RESULTS AND DISCUSSION
4.1 Effect of Pressure Drop on Permeate Flowrate for different Temperatures and Membrane Pore Sizes

The set of graphs below show the relationship between the exit flowrate and inlet pressure for each gas used in the experiment.
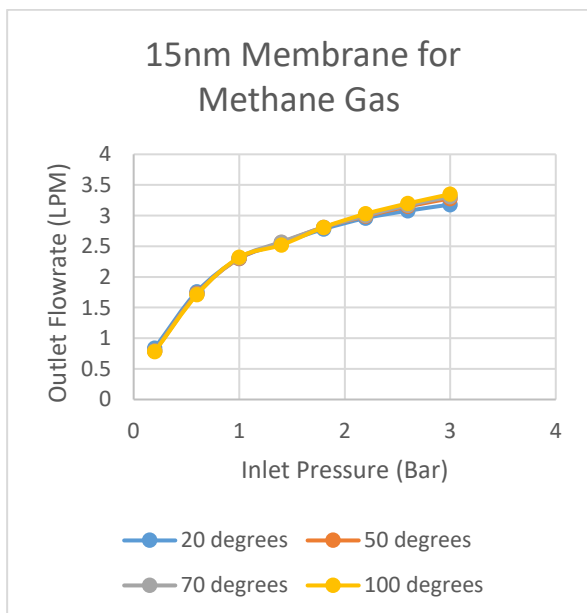
Figure 5 Effect of pressure drop on the flowrate of methane gas at various temperatures through a 15nm membrane
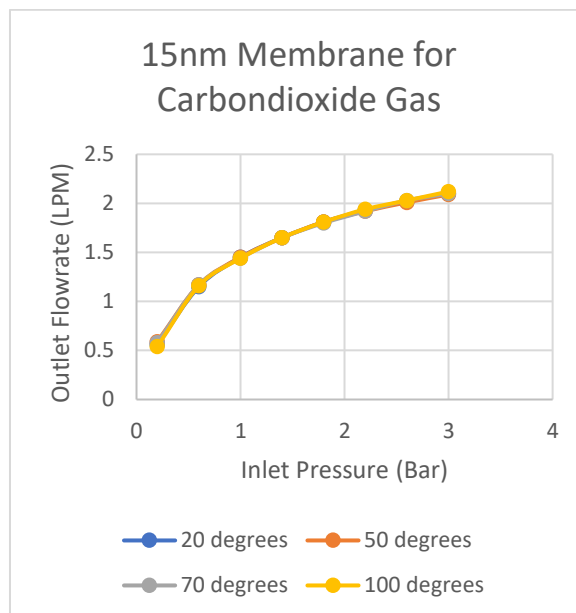

Figure 6 Effect of pressure drop on the flowrate of carbon dioxide gas at various temperatures through a 15nm membrane
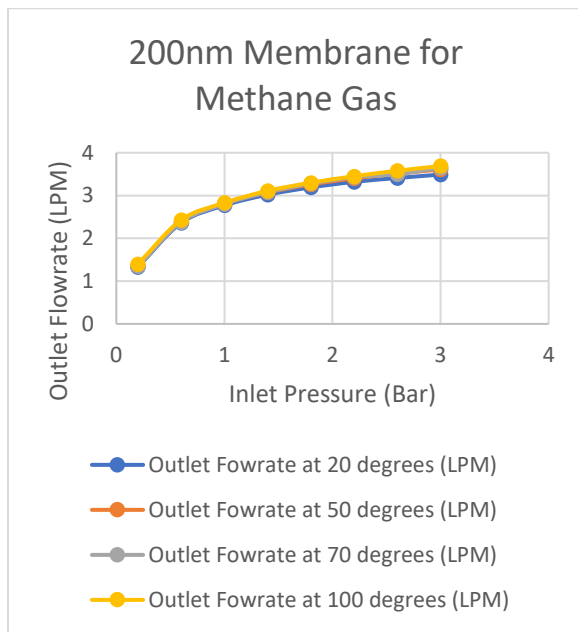
Figure 7 Effect of pressure drop on the flowrate of methane gas at various temperatures through a 200nm membrane
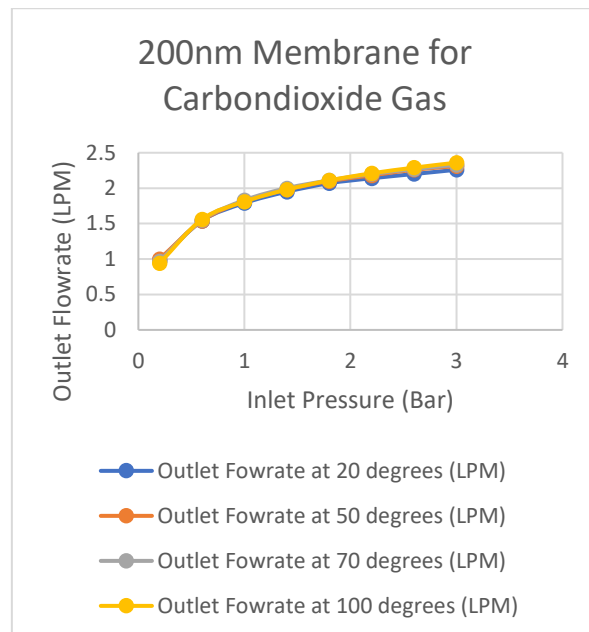

Figure 8 Effect of pressure drop on the flowrate of carbon dioxide gas at various temperatures through a 200nm membrane
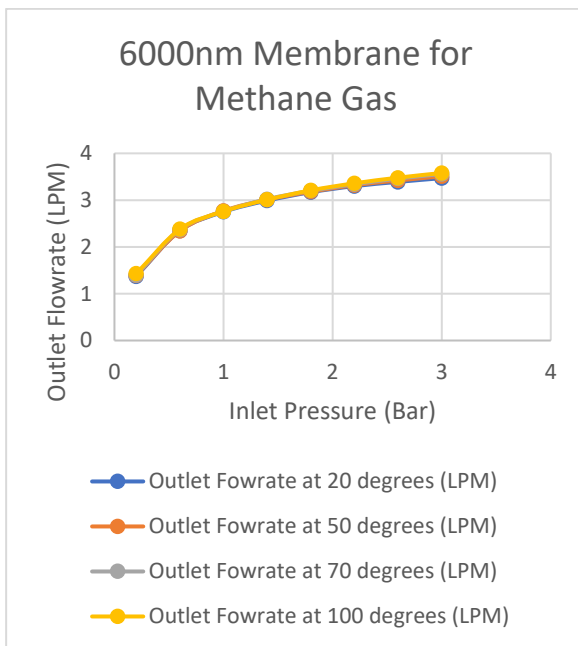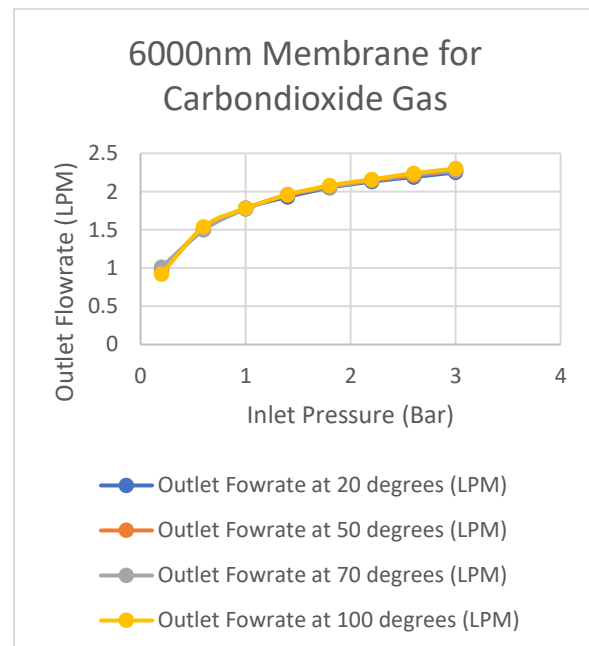

Figure 9 Effect of pressure drop on the flowrate of methane gas at various temperatures through a 6000nm membrane

Figure 10 Effect of pressure drop on the flowrate of carbon dioxide gas at various temperatures through a 6000nm membrane

From the figures above, we can note that at each pressure drop, the exit flowrate of each gas steadily increases with methane gas having a higher flowrate in each case. In terms of temperature, between 20 and 100 degrees celsius, the effect is negligible with no significant change in the exit flowrate of each gas.

4.2 Gas Comparison

The set of graphs below show a comparison of the effect of pressure drop on methane and carbon

dioxide outlet flowrate at set temperatures.
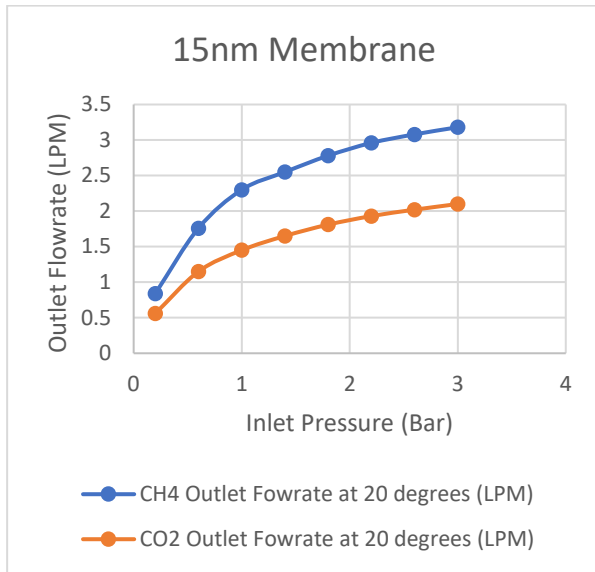
Figure 13 Effect of pressure drop on methane and carbon dioxide flowrate at 70 degrees through a 15nm membrane
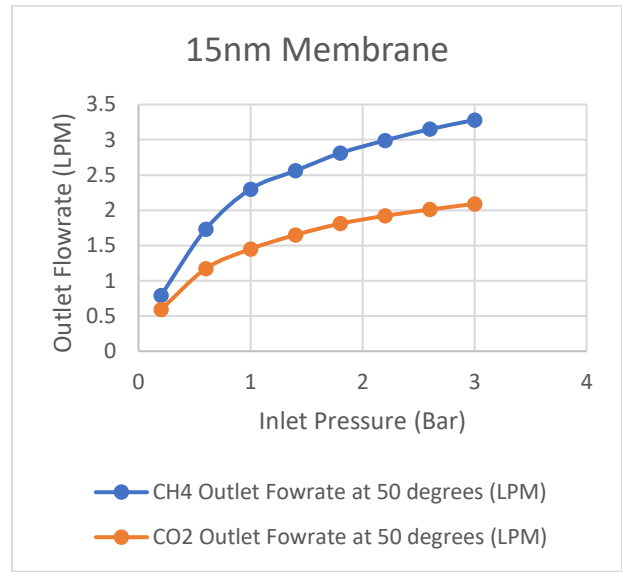
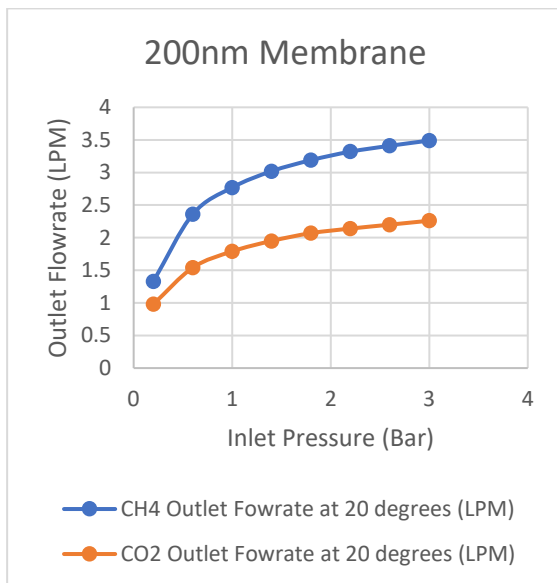Figure 14 Effect of pressure drop on methane and carbon dioxide flowrate at 100 degrees through a 15nm membrane

Figure 15 Effect of pressure drop on methane and carbon dioxide flowrate at 20 degrees through a 200nm membrane
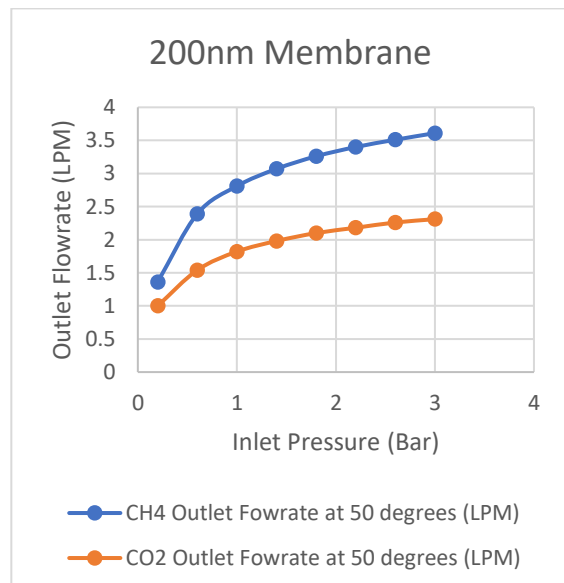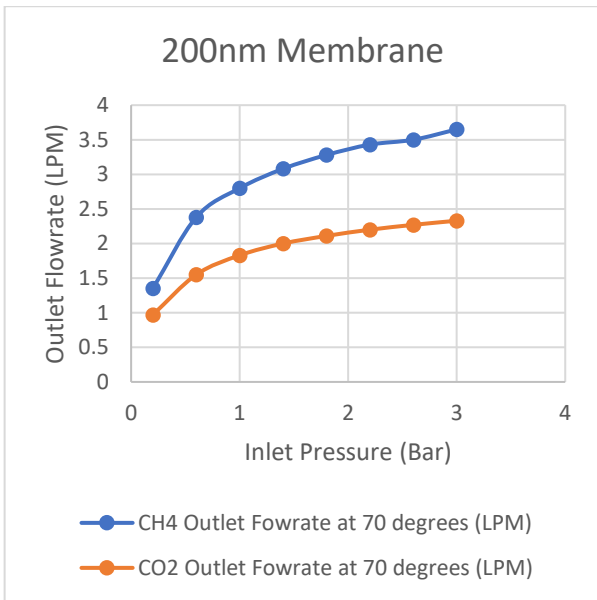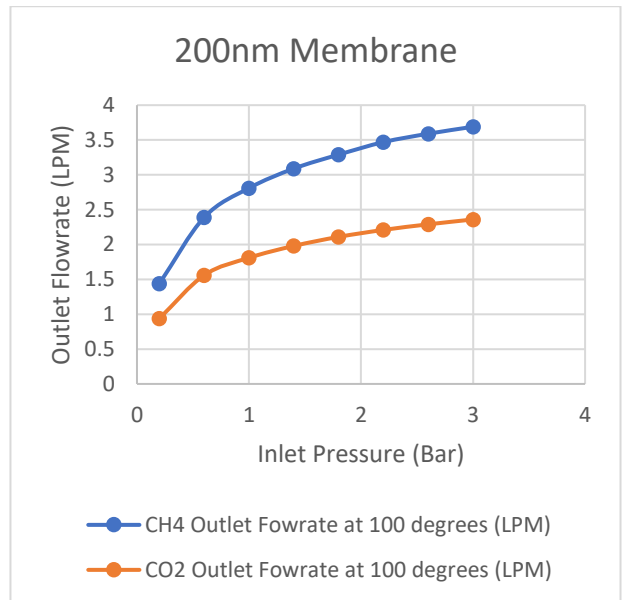

Figure 16 Effect of pressure drop on methane and carbon dioxide flowrate at 50 degrees through a 200nm membrane

Figure 17 Effect of pressure drop on methane and carbon dioxide flowrate at 70 degrees through a 200nm membrane

Figure 18 Effect of pressure drop on methane and carbon dioxide flowrate at 100 degrees through a 200nm membrane
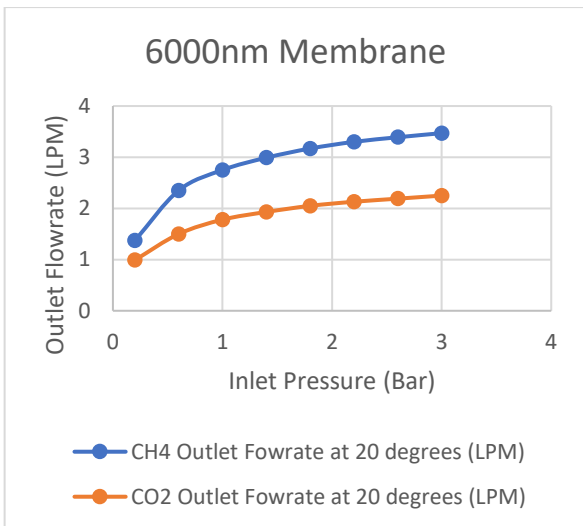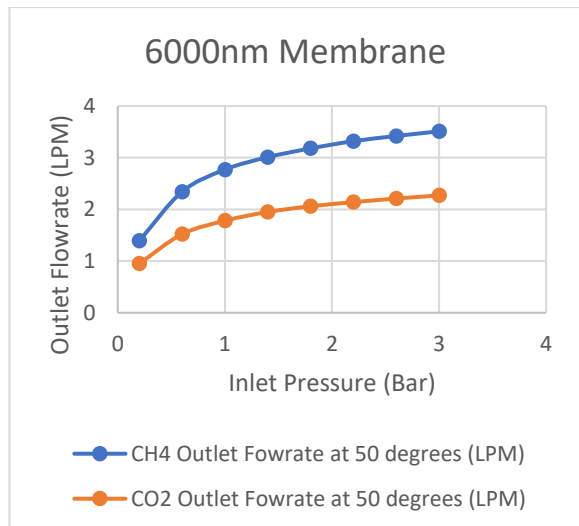

Figure 19 Effect of pressure drop on methane and carbon dioxide flowrate at 20 degrees through a 6000nm membrane

Figure 20 Effect of pressure drop on methane and carbon dioxide flowrate at 50 degrees through a 6000nm membrane
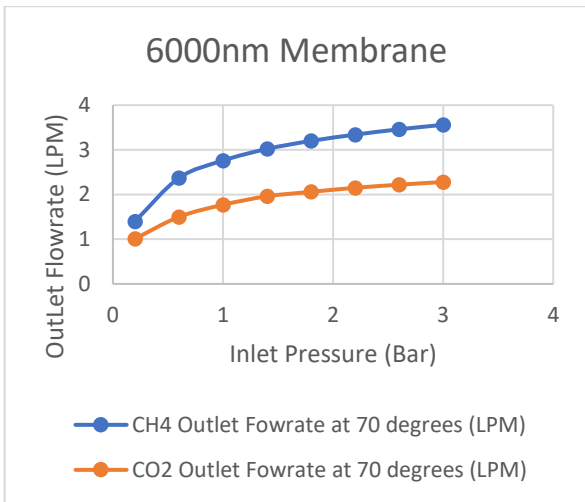
Figure 21 Effect of pressure drop on methane and carbon dioxide flowrate at 70 degrees through a 6000nm membrane
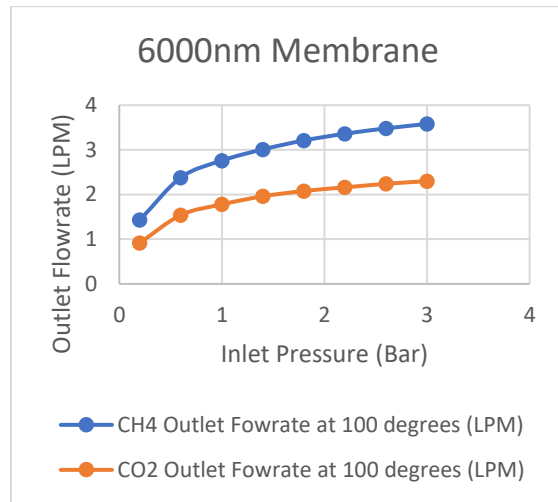
Figure 22 Effect of pressure drop on methane and carbon dioxide flowrate at 100 degrees through a 6000nm membrane

It can be observed from the figures above that the exit flowrate of each gas increases with increasing pore size. In the case of the 200nm and 6000nm membrane, methane and carbon dioxide gases show very high exit flowrate compare to the 15nm membranes, this is attributed to the large pores that allow carbon dioxide to flow along with methane without any restriction.

4.3 Gas Ratios

The following set of graphs show the relationship between pressure drop and the ratio of CH_4 and CO_2 gas flowrate at set temperatures.
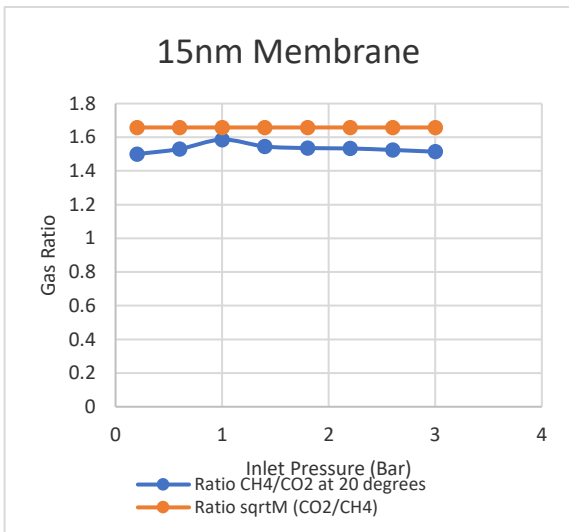

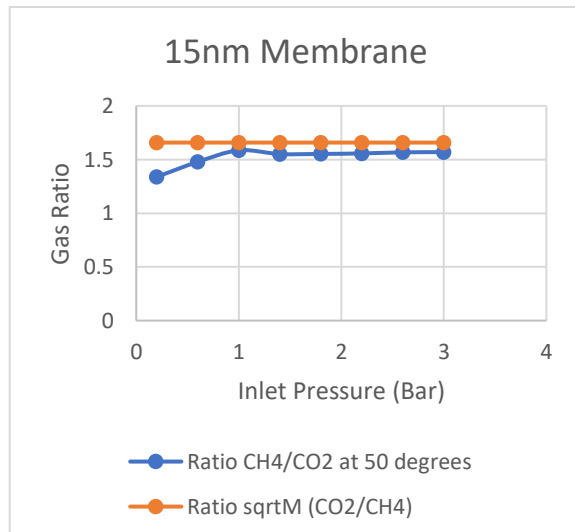Figure 23 Effect of pressure drop on gas ratios at 20 degrees through a 15nm membrane

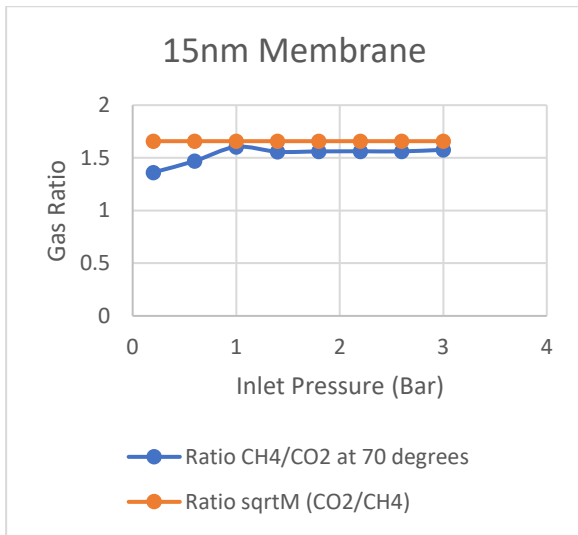Figure 24 Effect of pressure drop on gas ratios at 50 degrees through a 15nm membrane

Figure 25 Effect of pressure drop on gas ratios at 100 degrees through a 15nm membrane
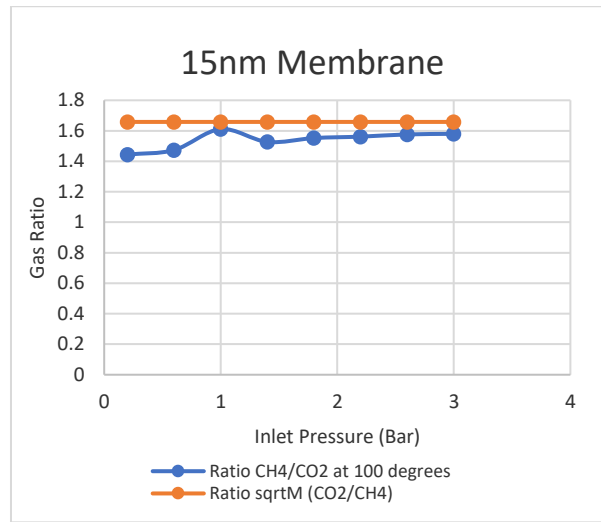

Figure 26 Effect of pressure drop on gas ratios at 100 degrees through a 15nm membrane
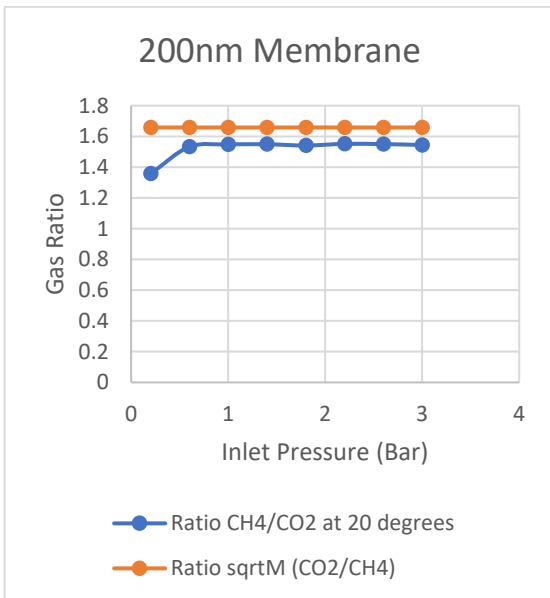

Figure 27 Effect of pressure drop on gas ratios at 20 degrees through a 200nm membrane

Figure 28 Effect of pressure drop on gas ratios at 50 degrees through a 200nm membrane

Figure 29 Effect of pressure drop on gas ratios at 70 degrees through a 200nm membrane

Figure 30 Effect of pressure drop on gas ratios at 100 degrees through a 200nm membrane

Figure 31 Effect of pressure drop on gas ratios at 20 degrees through a 6000nm membrane
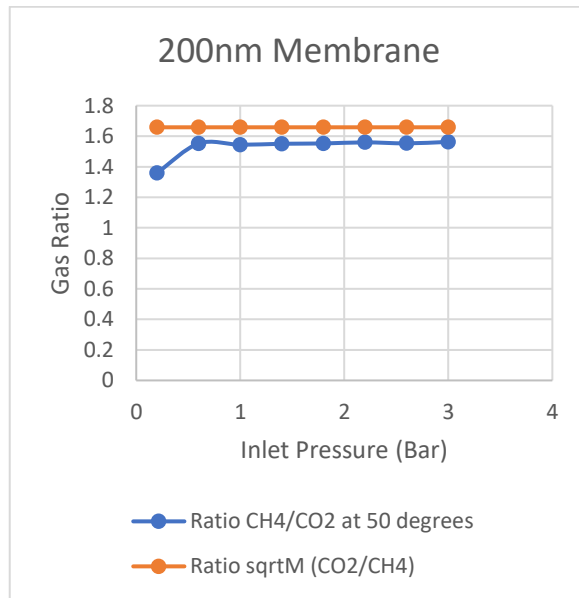

Figure 32 Effect of pressure drop on gas ratios at 50 degrees through a 6000nm membrane
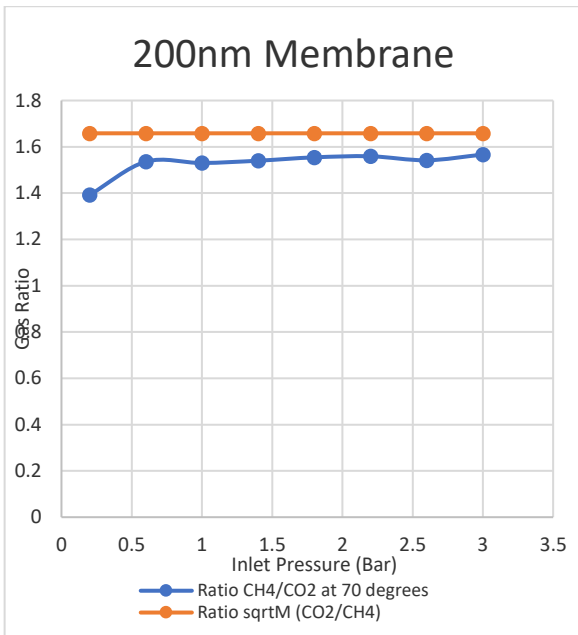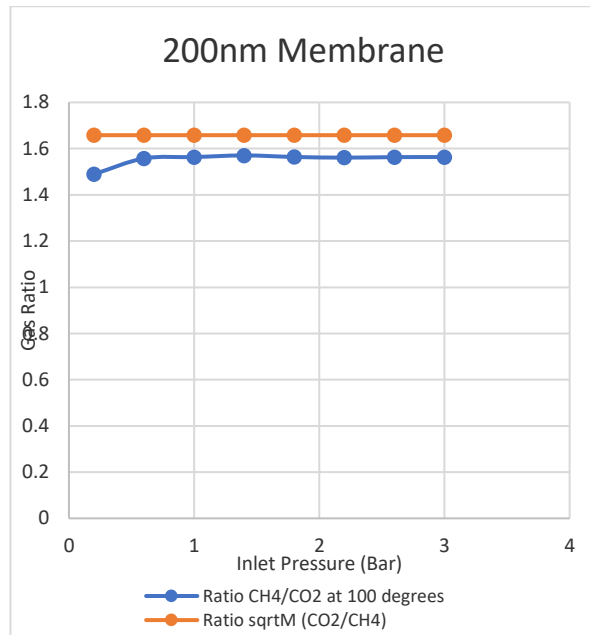
Figure 33 Effect of pressure drop on gas ratios at 70 degrees through a 6000nm membrane

Figure 34 Effect of pressure drop on gas ratios at 100 degrees through a 6000nm membrane
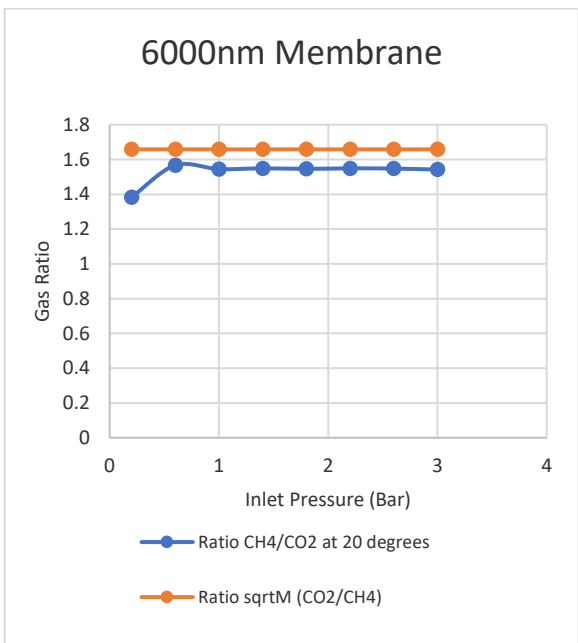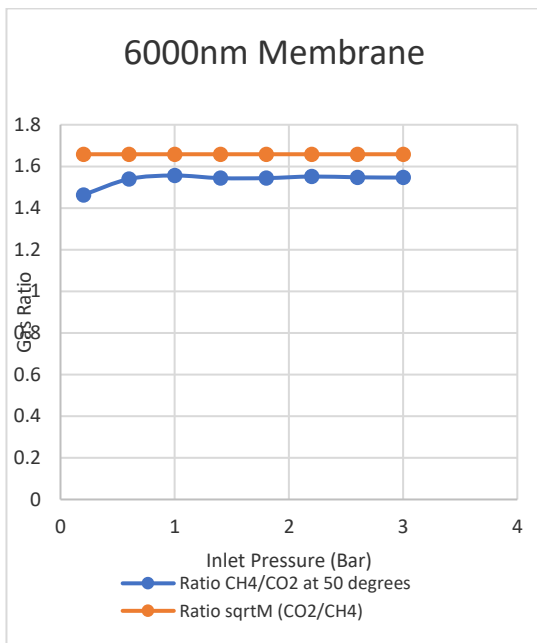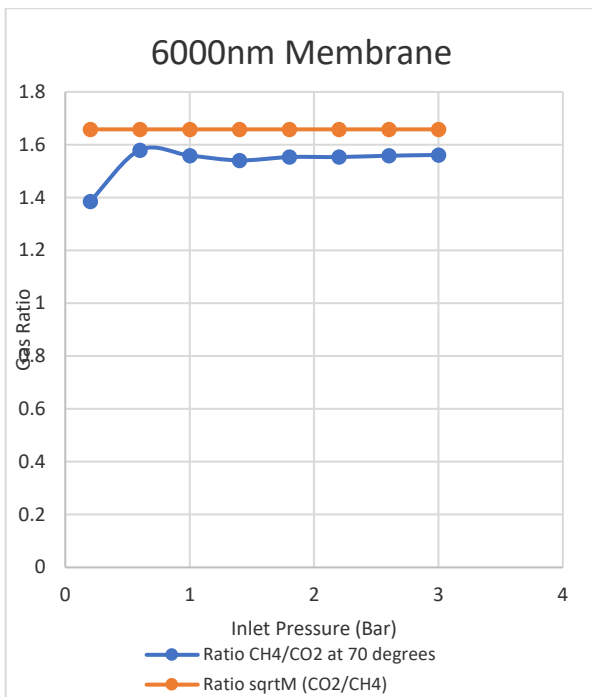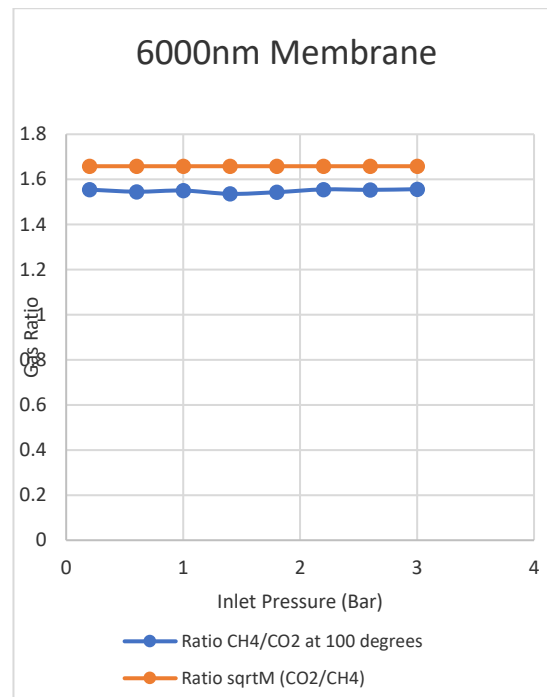
The figures above show that the 200nm and 6000nm membrane, which have very large pore sizes, does not approach ideality (i.e. the orange line depicting ratio of the square root of the molecular weight of gases) compared to the smaller sized 15nm membrane pores. Instead, the larger pore membranes show that the gases go farther and farther away from the ideal knudsen regime and show a viscous flow as described by Domenico in his findings (8). Thus, gas separation using this membrane would be very cumbersome compared to using membranes with smaller pore size.

It was observed that there was a proportional rise in flowrate as the pressure increased. Methane gas showed a higher exit flowrate than carbon dioxide irrespective of operating conditions, this indicates that the flux of methane through the membrane is greater than that of carbon dioxide in regular pore geometry and depicts a greater potential for upgrading of biogas which is a mixture of both. Results also show that flux is dependent on the gas molecular weight and viscosity as the heavier, more viscous gas, CO_2, did not pass through the membrane as quickly as the lighter, CH_4 gas. This agrees with Keizer et al.'s model that molecular size is a factor in considering the rate of permeation of gases (15,16).

It can also be deduced from these results that the 15nm membrane shows the greatest separation efficiency as the flux of CO_2 is restricted compared to CH_4; and the ratio of methane flowrate to carbon dioxide approaches the ideal knudsen regime. Consideration of reducing pore size, by modifying the membrane, would increase the efficiency of separation and a surface diffusion mechanism may be expected because the contact between gas molecules and the inner surface would be very strong.

5. CONCLUSIONS

Supplement to the depleting fossil fuels and increasingly stringent environmental regulation for greenhouse gases, this research proposes nano-structured membrane technology as an efficient means to transform biogas and shows good permeability characteristics, as well as offers chemical resistance, thermal and mechanical stability during operation. The other advantages of this technology include its compact size and minimal maintenance requirement making it attractive for use on offshore platforms.

The results from experiments show that molecular weight and viscosity of the gases also play a role

in their permeation rate as it approaches the Knudsen regime. In the case where the pore size is large compared to the molecular size of the gases, as in the 200nm and 6000nm membrane, there is viscous flow through the pores which is undesirable because no separation of gases can take place. However, where membrane of a smaller pore size is used, pressure drop across the membrane caused the gases to diffuse at different rates through the pores, this shows separation would take place. Thus, the project illustrates good utilization of the greenhouse gases present in biogas that would increase the heating value of the fuel making it easily adapted for other processes.

Ultimately, biogas upgrading technology can turn the cost of waste management into a revenue opportunity. Turning waste into a renewable source of energy by this upgrading process will reduce dependence on importation of fossil fuels, reduce greenhouse gas emissions, improve environmental quality, increase local jobs and provide revenue by export thereby boosting the economies. The benefits cannot be overstretched as even the digestate from anaerobic digestion offers an opportunity to recycle nutrients in the food supply, reducing the need for both petrochemical and mined fertilizers.

ORCID Id of authors
Ogunlude, Priscilla – 0000-0002-7365-8167
Abunumah, Ofasa – 0000-0003-4818-418X
Orakwe, Ifeyinwa – 0000-0003-3467-4604
Shehu, Habiba – 0000-0003-0834-162X
Muhammad-Sukki, Firdaus – 0000-0002-5415-2259
Gobina, Edward – 0000-0003-0769-9427

REFERENCES

Damle, A. (2014). An introduction to the utilization of membrane technology in the production of clean and renewable power. In *Membranes for Clean and Renewable Power Applications* (pp. 3–43). https://doi.org/10.1533/9780857098658.1.3

Domenico De Meis. (2017). *Gas-transport-through-porous-membranes*. Rome, Italy: Frascati Research Center.

Ghasemzadeh, K., Basile, A., & Iulianelli, A. (2019). Progress in Modeling of Silica-Based Membranes and Membrane Reactors for Hydrogen Production and Purification. *ChemEngineering*, *3*(1), 2. https://doi.org/10.3390/chemengineering3010002

Keizer, K., Burggraaf, A. J., Vroon, Z. A. E. P., & Verweij, H. (1998). Two component permeation through thin zeolite MFI membranes. *Journal of Membrane Science*, *147*(2), 159–172. https://doi.org/10.1016/S0376-7388(98)00133-1

Nagy, E. (2019). Chapter 3 - Mass Transport Through a Membrane Layer. In E. Nagy (Ed.), *Basic Equations of Mass Transport Through a Membrane Layer (Second Edition)* (pp. 21–68). https://doi.org/10.1016/B978-0-12-813722-2.00003-0

Oyama, S. T. (2011). Review on mechanisms of gas permeation through inorganic membranes. *Journal of the Japan Petroleum Institute*, *54*(5), 298–309.

Penev, M., Melaina, M., Bush, B., Muratori, M., Warner, E., & Chen, Y. (2016). *Low-Carbon Natural Gas for Transportation: Well-to-Wheels Emissions and Potential Market Assessment in California* (No. NREL/TP--6A50-66538, 1334743; p. NREL/TP--6A50-66538, 1334743). https://doi.org/10.2172/1334743

Rackley, S. A. (2017). 8 - Membrane separation systems. In S. A. Rackley (Ed.), *Carbon Capture and Storage (Second Edition)* (pp. 187–225). https://doi.org/10.1016/B978-0-12-812041-5.00008-8

Scarlat, N., Dallemand, J.-F., & Fahl, F. (2018). Biogas: Developments and perspectives in Europe. *Renewable Energy*, *129*, 457–472. https://doi.org/10.1016/j.renene.2018.03.006

Scott, K., & Hughes, R. (2012). *Industrial membrane separation technology*. Springer Science & Business Media.

Shehu, H., Okon, E., Orakwe, I., & Gobina, E. (2018). Design and Evaluation of Gas Transport through a Zeolite Membrane on an Alumina Support. In *Zeolites and Their Applications*. IntechOpen.

Svenskt Gastekniskt Center. (2012). *Basic data on biogas.* Malmö: Svenskt Gastekniskt Center.

Uchytil, P., Petrickovic, R., Thomas, S., & Seidel-Morgenstern, A. (2003). Influence of capillary condensation effects on mass transport through porous membranes. *Separation and Purification Technology*, *33*(3), 273–281. https://doi.org/10.1016/S1383-5866(03)00087-X

Uhlhorn, R. J. R., Keizer, K., & Burggraaf, A. J. (1992). Gas transport and separation with ceramic membranes. Part I. Multilayer diffusion and capillary condensation. *Journal of Membrane Science*, *66*(2), 259–269. https://doi.org/10.1016/0376-7388(92)87016-Q

Ullah Khan, I., Hafiz Dzarfan Othman, M., Hashim, H., Matsuura, T., Ismail, A. F., Rezaei-DashtArzhandi, M., & Wan Azelee, I. (2017). Biogas as a renewable energy fuel – A review of biogas upgrading, utilisation and storage. *Energy Conversion and Management*, *150*, 277–294. https://doi.org/10.1016/j.enconman.2017.08.035

Weinstein, B. L. (2019). Natural gas is the green new deal. Retrieved 20 May 2019, from San Antonio Express-News website: https://www.mysanantonio.com/opinion/commentary/article/Natural-gas-is-the-green-new-deal-13854946.php